Life Sciences 227 (2019) 64–73

Contents lists available at ScienceDirect

Life Sciences

journal homepage: www.elsevier.com/locate/lifescie

miR-27a promotes endothelial-mesenchymal transition in hypoxia-induced pulmonary arterial hypertension by suppressing BMP signaling

Ting Liu[a], Xiao-Zhou Zou[c], Ning Huang[a], Xiao-Yue Ge[a], Mao-Zhong Yao[a], Hong Liu[a], Zheng Zhang[a,b,*], Chang-Ping Hu[a,b,*]

[a] Department of Pharmacology, Xiangya School of Pharmaceutical Sciences, Central South University, Changsha, Hunan 410078, China
[b] Hunan Provincial Key Laboratory of Cardiovascular Research, Central South University, Changsha, Hunan 410078, China
[c] Department of Pharmacy, Zhejiang Provincial People's Hospital, Hangzhou, Zhejiang 310014, China

ARTICLE INFO

Keywords:
miR-27a
Smad5
Id2
Pulmonary arterial hypertension
Endothelial-mesenchymal transition

ABSTRACT

Aim: Growing evidence suggests that endothelial-mesenchymal transition (EndMT) play key roles in pulmonary arterial remodeling during pulmonary arterial hypertension (PAH), but the underlying mechanisms have yet to be fully understood. miR-27a has been shown to promote proliferation of pulmonary arterial cells during PAH, but its role in EndMT remains unexplored. This study was designed to investigate the role and underlying mechanism of miR-27a in EndMT during PAH.

Main methods: Rats were exposed in hypoxia (10% O_2) for 3 weeks to induce PAH, and human pulmonary artery endothelial cells (HPAECs) were exposed in hypoxia (1% O_2) for 48 h to induce EndMT. Immunohistochemistry, *in situ* hybridization, immunofluorescence, real-time PCR and Western blot were conducted to detect the expressions of RNAs and proteins, and luciferase assay was used to verify the putative binding site of miR-27a.

Key findings: We found that hypoxia up-regulated miR-27a in the tunica intima of rat pulmonary arteries and HPAECs, and that inhibition of miR-27a suppressed hypoxia-induced EndMT. Furthermore, elevated expression of miR-27a suppressed bone morphogenetic protein (BMP) signaling by targeting Smad5, thereby lessening Id2-mediated repression of the 2 critical mediators of EndMT (Snail and Twist).

Significance: Our data unveiled a novel role of miR-27a in EndMT during hypoxia-induced PAH. Thus, targeting of miR-27a-related pathway may be therapeutically harnessed to treat PAH.

1. Introduction

Pulmonary arterial hypertension (PAH) is a severe disease characterized by increased pulmonary vascular resistance and pulmonary artery pressure. It causes right ventricular failure and ultimately death [1,2]. Pulmonary arterial remodeling has been recognized as an important contributor to increased pulmonary artery pressure during the progression of PAH [3].

Recently, growing evidence suggests that endothelial-mesenchymal transition (EndMT) contributes greatly to pulmonary arterial remodeling in PAH [4]. During EndMT, endothelial cells undergo oval-to-spindle change in morphology; meanwhile, the endothelial markers (VE-cadherin, CD31) are decreased, while mesenchymal markers (Vimentin, α-SMA) are increased [4]. MicroRNAs (miRNAs) are a class of endogenous ~22 nucleotides-long small noncoding RNAs, which repress mRNA translation and/or promote its degradation by binding to the 3′-untranslated region (3′ UTR) of mRNA [5]. miR-27a, an inducer of epithelial-mesenchymal transition in cancers [6,7], has been implicated in the proliferation of pulmonary vascular cells during PAH [8–10]. Moreover, EndMT is considered as a specific case of epithelial-mesenchymal transition, suggesting that miR-27a might also participate in the regulation of EndMT in PAH.

Perturbed bone morphogenetic protein (BMP) signaling gives rise to various vascular diseases [11]; Mutation of the gene encoding BMPRII receptor and/or aberrant expression of other key components of BMP signal transduction (such as ALK1, Smad8 and BMP9) have been identified in patients with PAH [12–15]. Recently, reduced BMPRII has been demonstrated to trigger PAH by mechanistically promoting EndMT [16]. However, the question of whether the abnormal expression of other BMP signaling molecules could cause EndMT in PAH remains unanswered. Smad5, a pivotal effector of BMP signaling, has been found to be down-regulated in rat pulmonary arterial smooth

* Corresponding authors at: Department of Pharmacology, Xiangya School of Pharmaceutical Sciences, Central South University, No. 110 Xiangya Road, Changsha, Hunan 410078, China.
E-mail addresses: zzhang@csu.edu.cn (Z. Zhang), huchangping@csu.edu.cn (C.-P. Hu).

https://doi.org/10.1016/j.lfs.2019.04.038
Received 5 March 2019; Received in revised form 8 April 2019; Accepted 16 April 2019
Available online 17 April 2019
0024-3205/

muscle cells (PASMCs) in hypoxia-induced PAH [17]; however, evidence suggesting that Smad5 modulates EndMT in PAH is presently unavailable. Inhibitors of DNA binding proteins (Id) are the targets of Smad transcription factors [18] and participate in regulating the expression of Twist and Snail, both of which are critical mediators of EndMT [19–21]. Therefore, our hypothesis is that Smad5 would regulate EndMT *via* modulating Id proteins.

This study is designed to explore the role of miR-27a in hypoxia-induced EndMT in PAH. Our results demonstrate that miR-27a acts as a pro-EndMT factor by targeting Smad5 and consequently suppressing Id2.

2. Materials and methods

2.1. Animal experiments

Sprague-Dawley rats (male, 180–220 g) were purchased from the Experimental Animal Center of Central South University, China (SCXX (XIANG) 2009-0004). Animal experiments in this study were performed in compliance with the Guide of the Medicine Animal Welfare Committee of Xiangya School of Medicine, Central South University.

SD rat were kept in hypoxia at 10% O_2 for 3 weeks to induce PAH, and control rats were kept in normoxia for 3 weeks. Three weeks later, the right ventricle systolic pressure, the ratio of right ventricle weight to tibia length and the ratio of RV weight to left ventricle plus interventricular septum were measured and calculated to verify the PAH model. The fresh isolated pulmonary arteries and the right lower lobes of the lungs were used for the subsequent experiments.

2.2. Hematoxylin–eosin staining

The fresh right lower lobes of lungs were excised and fixed with 4% paraformaldehyde for 24 h, then the fixed tissues were embedded in paraffin and cut into slices with a thickness of 5 μm. Next, after dewaxing in xylene and rehydration in alcohol gradient, the slices were stained by hematoxylin and eosin to analyze the morphometric change of pulmonary artery.

2.3. Immunohistochemistry

Immunohistochemistry kit (SP-9000) was purchased from ZSGB-Bio (Beijing, China), and immunohistochemistry was conducted in accordance to manufacturer's instructions. After dewaxing and rehydration, the slices were placed into citrate antigen retrieval solution at 95 °C for 30 min to retrieve antigen. Next, the slices were permeabilized with Triton X-100 for 1 h and then incubated with 3% H_2O_2 deionized water to remove endogenous peroxidase for 10 min. After blocking with goat serum for 1 h, the slices were incubated with primary antibody at 4 °C overnight and then biotin-labeled secondary antibody at room temperature for 1 h. Finally, the slices were incubated with HRP-labeled streptomycin solution for 45 min at room temperature and developed with 3,3-diaminobenzidine (DAB) solution. The information of the primary antibodies was described in Table 1.

2.4. In situ hybridization

In situ hybridization kit was purchased from Boster (Wuhan, China), and *in situ* hybridization was conducted according to the manufacturer's instructions. After dewaxing and rehydration, the slices were incubated with 3% citric acid solution containing pepsin at room temperature for 15 min to expose the interest RNA. Then, 1% paraformaldehyde was used to fix the slices. After fixation, the slices were incubated with prehybridization solution for 4 h at 37 °C to decrease background. Next, the slices were incubated with hybridization solution at 37 °C overnight and washed with 2× saline sodium citrate (SSC) solution (10 × SSC: 1.5 M NaCl, 0.15 M Na-citrate, pH 7.0), 0.5 × SSC and 0.2 × SSC in turn. After washing, the slices were blocked with blocking buffer and incubated with biotin-labeled digoxin at 37 °C for 1 h. Finally, the slices were incubated with streptavidin-biotin complex and avidin-biotin-peroxidase in turn and developed with 3,3-diaminobenzidine solution.

2.5. Cell culture and treatment

Human pulmonary artery endothelial cells (HPAECs) (3100, ScienCell) were purchased from ScienCell Research Laboratories (San Diego, USA). The cells were cultured in Endothelial Cell Medium (ECM) (1001, ScienCell) with 5% fetal bovine serum (FBS) (0025, ScienCell), 1% Endothelial Cell Growth Supplement (1052, ScienCell) and 1% Penicillin/Streptomycin Solution (0503, ScienCell) at 37 °C under 5% CO_2. Before treatment, the cells were cultured in ECM with 1% FBS for 24 h to synchronize cells. Then, hypoxia groups were cultured in hypoxia (1% O_2) for 48 h and control groups were cultured in normoxia.

2.6. Cell transfection

miR-27a inhibitor and mimic were purchased from RiboBio (Guangzhou, China), Smad5-expressing and Id2-expressing plasmids were constructed and synthesized by Genechem (Shanghai, China). Ribo FECT™ CP transfection kit was used to transfect inhibitor, mimic or plasmids into cells according to the manufacturer's instructions. After transfection for 24 h, cells were used for the further experiments. The working concentration of miR-27a inhibitor, miR-27a mimic, Smad5-expressing plasmids and Id2-expressing plasmids were 200 nM, 50 nM, 150 ng/ml and 100 ng/ml, respectively.

2.7. Immunofluorescence

For lung tissues, after dewaxing and rehydration, the slices were placed into citrate antigen retrieval solution at 95 °C for 30 min to retrieve antigen. Then, the slices were permeabilized with Triton X-100 for 1 h. After blocking with goat serum for 1 h, the slices were incubated with the first specific primary antibodies at 4 °C overnight and subsequently incubated with Cy3-labeled goat anti-rabbit IgG (P0183, Beyotime, Shanghai, China) at room temperature for 1 h. Then, the slices were washed with PBS and incubated with the anti-CD31 antibody at 4 °C overnight and subsequently incubated with FITC-labeled goat anti-mouse IgG (P0196, Beyotime, Shanghai, China) at room temperature for 1 h. Finally, the slices were washed with PBS and observed under the fluorescence microscopy. The information of the primary antibodies was described in Table 1.

For cells, after treatments, the cells were washed and fixed with 4% paraformaldehyde. After blocking with 5% bovine serum album (BSA), the cells were incubated with the first specific primary antibodies (Table 1) at 4 °C overnight and subsequently incubated with the secondary fluorescent antibody (Cy3 or FICT) at room temperature. Finally, the cells were observed under the fluorescence microscopy.

2.8. Real-time PCR

RNAiso Plus (9108, TaKaRa, Beijing, China) was used to extract total RNA in from pulmonary artery and HPAECs. PrimeScript™ RT reagent Kit (RR037A, TaKaRa, Beijing, China) was used for RNA reverse transcription. The reverse transcription primers and real-time PCR primers of miR-27a were purchased from RiboBio (Guangzhou, China), real-time PCR primers of Smad5 and β-actin mRNA were synthesized by Sangon Biotech (Shanghai, China). TB Green™ *Premix Ex Taq*™ (RR420A, TaKaRa, Beijing, China) was used for quantitative analysis of miRNAs and mRNAs *via* ABI Prism 7300 system (Applied Biosystems). The PCR conditions refer to the TB Green™ *Premix Ex Taq*™ instructions. β-actin and U6 were used as endogenous controls of mRNA and miRNAs, respectively. Smad5 forward, TCTTTAGATGGACGCCTGCA and reverse, TCATTGTGGCTCAGGTTCCT; β-actin forward, TGACGTG

Table 1
The information of the primary antibodies.

Anti-bodies	Brand	Cat. no.	Source	Dilution ratio	Application
CD31	Abcam	ab119339	Mouse	IF: 1:100	IF
CD31	Santacruz	sc-376764	Mouse	WB: 1:200	WB
Vimentin	Abcam	ab92547	Rabbit	WB: 1:1000, IF/IHC: 1:200	WB, IF, IHC
a-SMA	Abcam	ab32575	Rabbit	WB: 1:1000, IF/IHC: 1:200	WB, IF, IHC
Smad5	Abcam	ab40771	Rabbit	WB: 1:500, IF/IHC: 1:50	WB, IF, IHC
p-Smad5	Abcam	ab92698	Rabbit	WB: 1:500, IHC: 1:50	WB, IHC
Id2	Abcam	ab166708	Mouse	WB: 1:500	WB
Id2	Abcam	ab217551	Rabbit	IHC: 1:100	IHC
Snail	Abcam	ab53519	Goat	WB: 1:500, IHC: 1:100	WB, IHC
Twist	Abcam	ab50581	Rabbit	WB: 1:1000, IHC: 1:400	WB, IHC
Twist	Proteintech	25465-1-AP	Rabbit	IP: 4 μg/1 mg total protein	IP
E2A	Proteintech	21242-1-AP	Rabbit	WB: 1:500	IP
β-actin	Beyotime	AF0003	Mouse	WB: 1:1000	WB

GACATCCGCAAAG and reverse, CTGGAAGGTGGACAGCGAGG.

2.9. Western blot

RIPA Lysis Buffer (P0013B, Beyotime, Shanghai, China) with 0.1% PMSF was used to extract total protein. BCA Protein Assay Kit (P0010, Beyotime, Shanghai, China) was used to measure the protein concentration. After denaturation, proteins were separated by 8/10/15% SDS-PAGE (depended on the molecular weight of the interest protein) and then transferred to polyvinylidene fluoride membranes. After blocking with 5% BSA, the membranes were incubated with primary antibodies at 4 °C overnight and then incubated with the HRP-labeled secondary antibody at room temperature for 1 h. The chemiluminescence signals were developed with the BeyoECL Star (P0018AS, Beyotime, Shanghai, China) and analyzed by ChemiDoc XRS + system (Bio-Rad Co. Ltd. USA). β-actin was used as an endogenous control. The information of the primary antibodies was described in Table 1.

2.10. Co-immunoprecipitation

1 mL whole cell lysate with 1000 μg protein was prepared first. Then, 4 μg anti-Twist antibody was added into the whole cell lysate for pulling down the interest complexes. After incubation overnight at 4 °C, 30 μL protein A agarose (P2006, Beyotime, Shanghai, China) was added into the whole cell lysate for collecting the complexes. After incubation for 4 h at 4 °C, the protein A agarose was collected and then mixed with RIPA buffer containing 1 × SDS for denaturation. Finally, Western blot was conducted to examine the expression of E2A. The information of the primary antibodies was described in Table 1.

2.11. Luciferase assay

The 3′ UTR of Smad5 mRNA with putative/mutant miR-27a binding site was cloned into pmiR-RB-Report™ Vector (Ribobio, Guangzhou, China). Renilla luciferase (Rluc) acts as a reporter, and firefly luciferase (Luc) acts as a control. HPAECs grown in 96-well plates were co-transfected with the Vector (2 μg) and miR-27a mimic (50 nM) by ribo FECT™ CP transfection kit. After incubation for 48 h, renilla and firefly luciferase activities was detected with Dual-Luciferase® Reporter Assay System (E1910, Promega).

2.12. Statistical analysis

SPSS software (Version 19.0) was used for statistical analysis. Data were expressed as mean ± S.E.M. Statistical analysis was performed by unpaired Student's *t*-test for two groups; One-way ANOVA followed by Newman-Student-Keuls test was performed for multiple groups. Differences were considered statistically significant when $P < 0.05$.

3. Results

3.1. Hypoxia induced PAH and EndMT in vivo and in vitro

This study is designed to explore whether miR-27a mediates hypoxia-induced EndMT in PAH *via* repressing BMPs signal by targeting Smad5. To induce PAH, rats were exposed to hypoxia (10% O_2) for 3 weeks. Right ventricle systolic pressure, ratio of right ventricle weight to tibia length and ratio of RV weight to left ventricle plus interventricular septum were all significantly increased (25.2 ± 0.48 *vs* 42.8 ± 1.43, 0.042 ± 0.002 *vs* 0.075 ± 0.002 and 0.188 ± 0.007 *vs* 0.434 ± 0.015, respectively) in hypoxia-exposed rats (Fig. 1a); meanwhile, the thickness of pulmonary artery wall in hypoxia group was increased markedly (Fig. 1b). These results indicate that rats exposed to hypoxia suffered from PAH.

To examine whether endothelial cells undergo EndMT, double-labelling immunofluorescence was conducted. As revealed (Fig. 1c), in pulmonary arteries of hypoxia-induced PAH rats, PAECs expressed α-SMA (a mesenchymal marker), which was absent in control rats. Meanwhile, the expression of CD31 (an endothelial marker) was down-regulated (1.000 ± 0.000 *vs* 0.245 ± 0.050), whereas the expression of both α-SMA and Vimentin (another mesenchymal marker) was up-regulated (1.000 ± 0.000 *vs* 1.598 ± 0.161 and 1.000 ± 0.000 *vs* 2.674 ± 0.339, respectively) in pulmonary arteries of hypoxia-exposed rats (Fig. 1d). Additionally, HPAECs acquired the mesenchymal-like phenotypes after exposure to hypoxia (Fig. 1e). These results indicated that hypoxia induced mesenchymal transition of PAECs *in vivo* and *in vitro*.

3.2. miR-27a promoted hypoxia-induced EndMT

miR-27a has been shown to be up-regulated in pulmonary arteries in PAH [8,9]. In this study, we further verified its up-regulation (1.157 ± 0.115 *vs* 1.843 ± 0.129) in pulmonary arteries in hypoxia-induced PAH; *In situ* hybridization revealed that miR-27a was up-regulated considerably in the tunica intima of pulmonary arteries (Fig. 2a). Consistently, after *in vitro* exposure to hypoxia, miR-27a in HPAECs was also up-regulated (1.212 ± 0.109 *vs* 1.590 ± 0.129) (Fig. 2b).

To explore whether miR-27a mediates hypoxia-induced EndMT, miR-27a inhibitor was transfected into HPAECs before exposure to hypoxia. As shown in Fig. 2c–e, miR-27a inhibitor efficaciously suppressed the expression of miR-27a (1.041 ± 0.105 *vs* 0.013 ± 0.002); and it reversed hypoxia-induced increase in both Vimentin and α-SMA (1.729 ± 0.024 *vs* 0.888 ± 0219 and 1.541 ± 0.149 *vs* 0.934 ± 0.087, respectively), hypoxia-induced decrease in CD31 (0.622 ± 0.013 *vs* 0.917 ± 0.112), as well as the morphological change of HPAECs. Additionally, as shown in Fig. 2f–h, miR-27a mimic up-regulated the expression of miR-27a (1.108 ± 0.070 *vs*

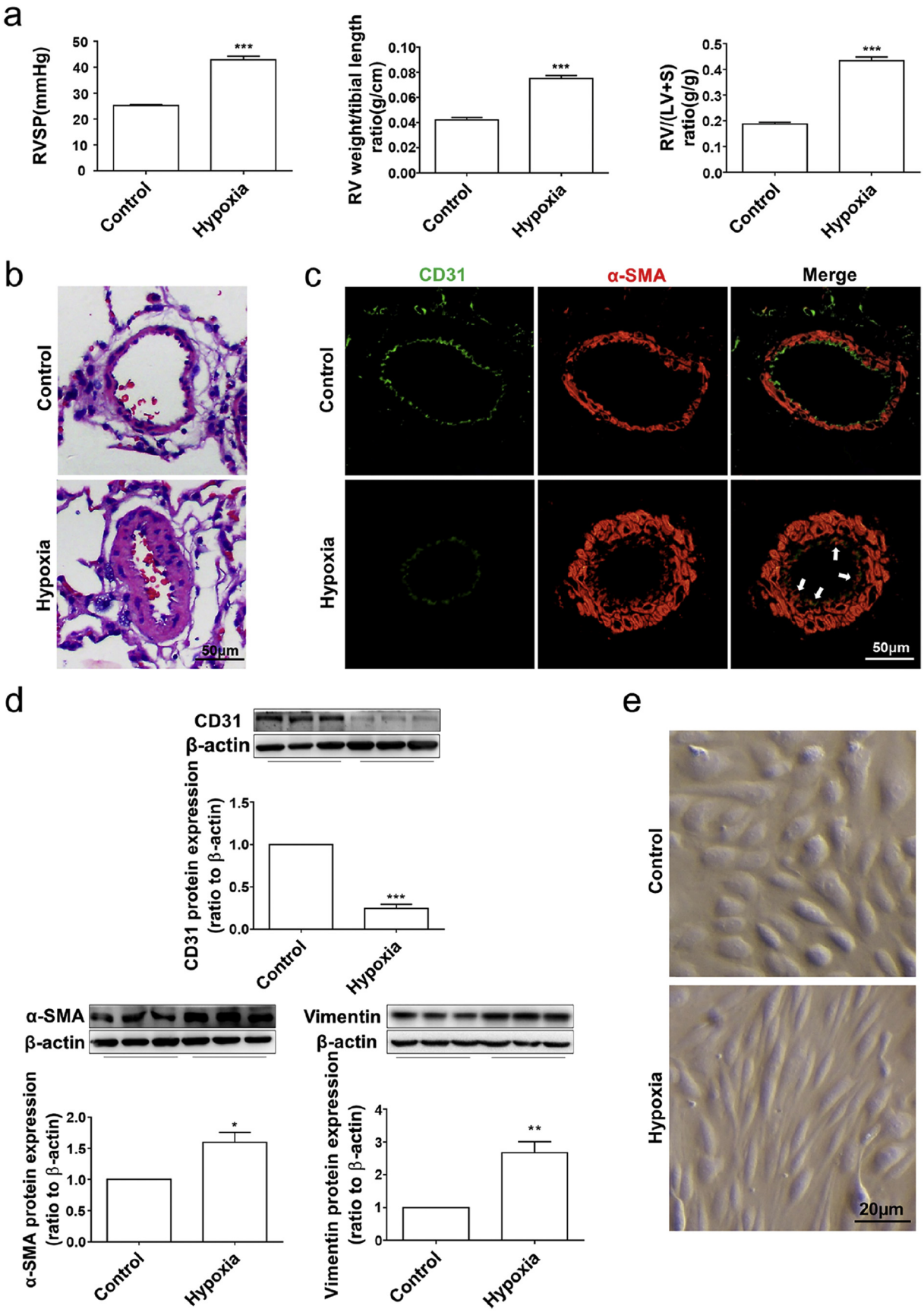

Fig. 1. Hypoxia induced PAH and EndMT *in vivo* and *in vitro*. (a) RVSP, RV/tibia length and RV/(LV + IS) in each group (n = 10). (b) Hematoxylin–eosin staining in rat pulmonary artery. (c) The expression of both CD31 and α-SMA in rat pulmonary artery detected by double-labelling immunofluorescence; the arrows indicated that hypoxia induced the expression of α-SMA in the tunica intima of rat pulmonary artery. (d) The expression of CD31, Vimentin and α-SMA in rat pulmonary artery detected by Western blot (n = 3). (e) The morphologic change of HPAECs after exposure to hypoxia for 48 h. RVSP, right ventricle systolic pressure; RV, right ventricle; LV, left ventricle; IS, interventricular septum. Data are mean ± S.E.M. $^{*}P < 0.05$, $^{**}P < 0.01$, $^{***}P < 0.001$ compared with Control.

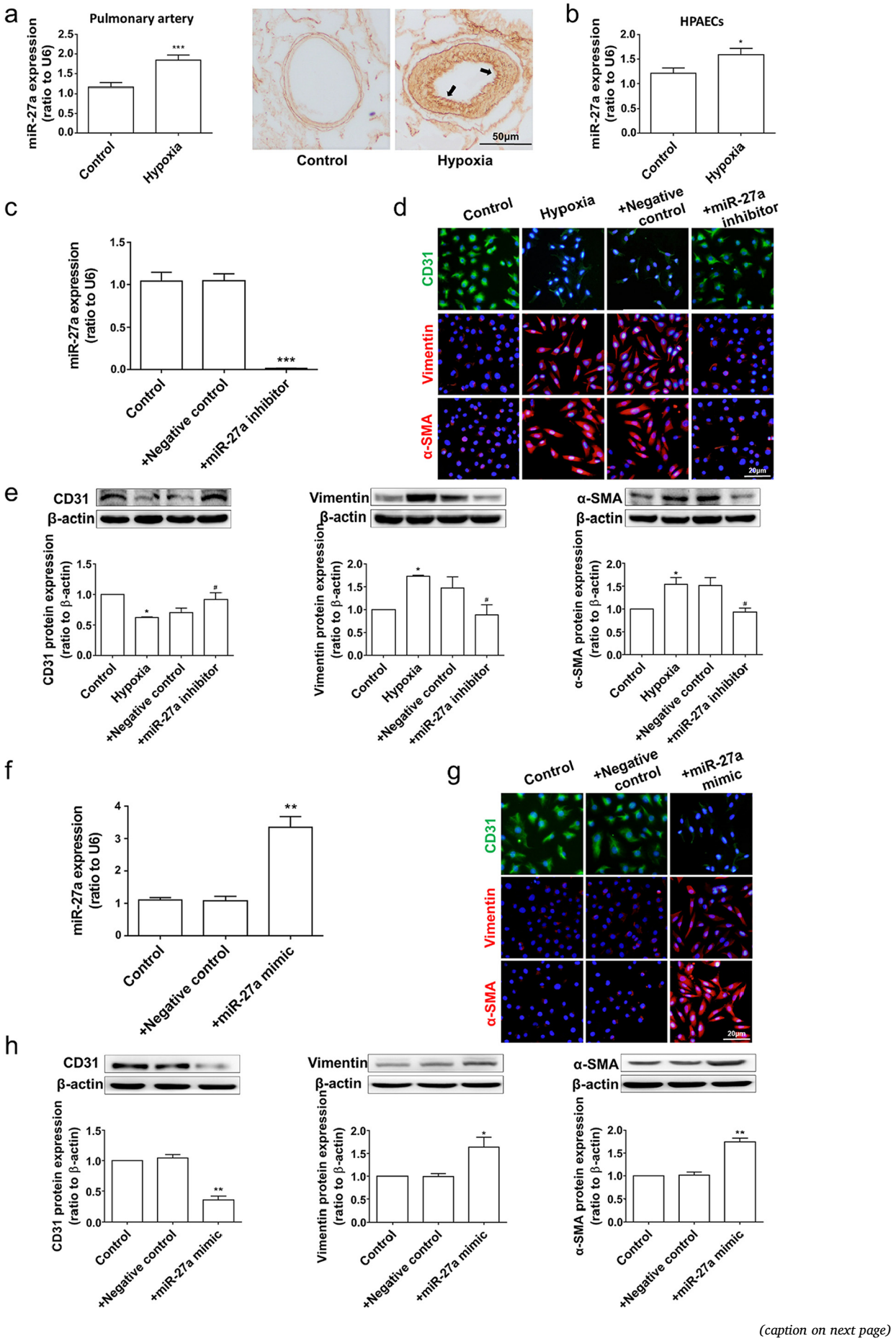

(caption on next page)

Fig. 2. miR-27a promoted hypoxia-induced EndMT. (a) The expression of miR-27a in rat pulmonary artery detected by *in situ* hybridization and real-time PCR (n = 3); the arrows indicated the expression of miR-27a in the tunica intima of pulmonary artery. (b) The expression of miR-27a in HPAECs detected by real-time PCR (n = 3). (c) The efficiency of miR-27a inhibitor in HPAECs detected by real-time PCR (n = 3). (d) The expression of CD31, Vimentin and α-SMA in hypoxia-induced HPAECs after miR-27a inhibitor transfection detected by immunofluorescence. (e) The expression of CD31, Vimentin and α-SMA in hypoxia-induced HPAECs after miR-27a inhibitor transfection detected by Western blot (n = 3). (f) The efficiency of miR-27a mimic in HPAECs detected by real-time PCR (n = 3). (g) The expression of CD31, Vimentin and α-SMA in HPAECs after miR-27a mimic transfection detected by immunofluorescence. (h) The expression of CD31, Vimentin and α-SMA in HPAECs after miR-27a mimic transfection detected by Western blot (n = 3). Data are mean ± S.E.M. $^{*}P < 0.05$, $^{**}P < 0.01$ compared with Control, $\#P < 0.05$ compared with Hypoxia.

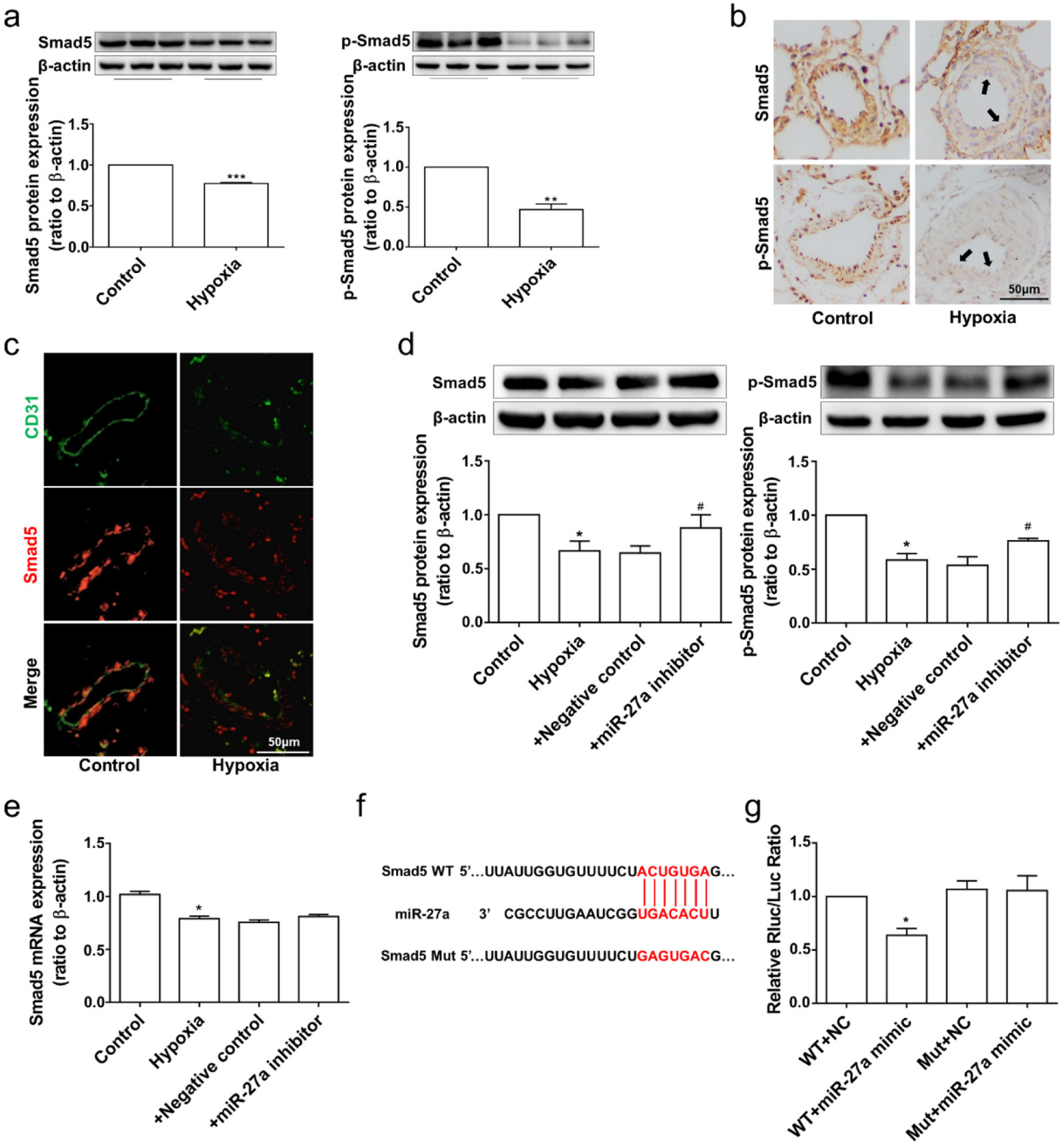

Fig. 3. Smad5 is a target of miR-27a in hypoxia-induced EndMT. (a) The expression of both Smad5 and p-Smad5 in rat pulmonary artery detected by Western blot (n = 3). (b) The expression of both Smad5 and p-Smad5 in rat pulmonary artery detected by immunohistochemistry; the arrows indicated the expression of both Smad5 and p-Smad5 in the tunica intima of pulmonary artery. (c) The expression of both Smad5 and CD31 in rat pulmonary artery detected by double-labelling immunofluorescence. (d) The expression of both Smad5 and p-Smad5 in hypoxia-induced HPAECs after miR-27a inhibitor transfection detected by Western blot (n = 3). (e) The expression of Smad5 mRNA in hypoxia-induced HPAECs after miR-27a inhibitor transfection detected by real-time PCR (n = 3). (f) The putative binding site of miR-27a in 3′ UTR of Smad5 mRNA, and the mutant 3′ UTR of Smad5 mRNA. (g) Luciferase analysis for examining whether miR-27a targets 3′ UTR of Smad5 mRNA (n = 3). Rluc acts as a reporter and Luc acts as a control, Rluc/Luc ratio indicates the relative luciferase activity of Smad5 mRNA. WT, wild type; Mut, mutant. NC, negative control. $^{*}P < 0.05$, $^{**}P < 0.01$, $^{***}P < 0.001$ compared with Control or WT + NC, $\#P < 0.05$ compared with Hypoxia. Data are mean ± S.E.M.

3.347 ± 0.335), and induced HPAECs to acquire the phenotype of mesenchymal-like cells. These results indicated that hypoxia-induced up-regulation of miR-27a *in vivo* and *in vitro* promoted EndMT in hypoxia-induced PAH.

3.3. Smad5 is a target of miR-27a in hypoxia-induced EndMT

It is well known that BMP signals play critical roles in PAH and Smad5 is a key effector in BMP signaling [11]. To investigate whether Smad5 contributes to hypoxia-induced EndMT, the abundance of total Smad5 and phosphorylated Smad5 (p-Smad5, the activated form of Smad5) [22] in rat pulmonary arteries were examined. As shown in Fig. 3a, both Smad5 and p-Smad5 were down-regulated (1.000 ± 0.000 *vs* 0.773 ± 0.013 and 1.000 ± 0.000 *vs* 0.468 ± 0.070, respectively) in abundance in pulmonary arteries of hypoxia-treated rats. Moreover, immunohistochemistry and immunofluorescence revealed that the down-regulation of both Smad5 and p-Smad5 occurred principally in the intima of pulmonary arteries (Fig. 3b and c).

Bioinformatic analysis predicted that Smad5 would be a target of miR-27a. To experimentally validate, miR-27a inhibitor was transfected into HPAECs. As shown, inhibition of miR-27a reversed hypoxia-induced protein down-regulation of both Smad5 and p-Smad5 (0.605 ± 0.071 *vs* 0.886 ± 0.104 and 0.586 ± 0.058 *vs* 0.763 ± 0023, respectively) (Fig. 3d), but exerted no discernable effects on Smad5 mRNA (0.791 ± 0.022 *vs* 0.809 ± 0.021) (Fig. 3e). To explore whether miR-27a targets 3′ UTR of Smad5 mRNA, we mutated the putative binding site (Fig. 3f). As shown in Fig. 3g, miR-27a mimic reduced the luciferase activity in cells transfected with construct containing wild-type Smad5 3′ UTR (1.000 ± 0.000 *vs* 0.638 ± 0.065), whereas luciferase activity was unchanged using 3′ UTR binding sites-mutated construct. These results indicated that miR-27a repressed the translation of Smad5 mRNA by binding to its 3′ UTR.

3.4. Overexpression of Smad5 up-regulated Id2 and thereby down-regulated Snail and Twist

Id2 has been demonstrated to be decreased in PASMCs in hypoxia-induced and familial PAH [17,23]. In this study, Id2 was verified to be down-regulated (1.000 ± 0.000 *vs* 0.581 ± 0.105) in pulmonary arteries in hypoxia-induced PAH rats (Fig. 4a), and immunohistochemistry revealed that hypoxia induced down-regulation of Id2 was most pronounced in the intimal layers (Fig. 4b). To investigate whether Id2 is a target of Smad5, Smad5-expressing plasmid was transfected into HPAECs. As shown in Fig. 4c, heterologous expression of Smad5 reversed hypoxia-induced down-regulation of both Smad5 and p-Smad5 (0.562 ± 0.059 *vs* 1.095 ± 0.063 and 0.587 ± 0.116 *vs* 0.970 ± 0.046, respectively). Meanwhile, hypoxia-induced down-regulation of Id2 was also reversed (0.590 ± 0.065 *vs* 0.782 ± 0.042) by Smad5 overexpression (Fig. 4d).

Snail and Twist are crucial pro-EndMT transcription factors [24]. In the present study, we found that both Snail and Twist were up-regulated (1.000 ± 0.000 *vs* 1.490 ± 0.109 and 1.000 ± 0.000 *vs* 1.711 ± 0.216, respectively) in pulmonary arteries in hypoxia (Fig. 4e), which occurred in the intima of pulmonary arteries as revealed by immunohistochemistry (Fig. 4f). To see whether Id2 modulates the expression of Snail and Twist, Id2 was heterologously expressed in HPAECs. As shown in Fig. 4g, hypoxia-induced down-regulation of Id2 was reversed (0.490 ± 0.065 *vs* 1.122 ± 0.065) in cells transfected with Id2-expressing plasmid. Meanwhile, hypoxia-induced up-regulation of both Snail and Twist were reversed (1.743 ± 0.217 *vs* 1.015 ± 0.147 and 1.764 ± 0.042 *vs* 0.722 ± 0.095, respectively) upon Id2 overexpression (Fig. 4h). Twist belongs to helix-loop-helix transcription factors and initiates transcription by assembling with E-proteins and then binding to the E-box of target genes [25]. Id proteins repress transcriptional activity and stability of Twist by competitively binding with E-proteins [20,25]. To validate, co-immunoprecipitation analysis was conducted. As shown in Fig. 4i, Twist bound to E2A (a ubiquitous E-protein), and overexpression of Id2 suppressed hypoxia-induced up-regulation of Twist-E2A complex. There results suggest that Smad5 mediated EndMT by modulating Id2.

4. Discussion

PAH is a devastating cardiovascular disease with high mortality and poor prognosis. Pulmonary arterial remodeling, the underlying pathological basis of increased pulmonary vascular resistance and pulmonary artery pressure, eventually causes right ventricular failure and death [1,2]. EndMT, an intriguing and important pathological process, plays a key role in pulmonary arterial remodeling during PAH. [4]. In this study, we demonstrated, for the first time, the role of miR-27a in EndMT during hypoxia-induced PAH. Mechanistically, miR-27a suppressed BMP signaling by targeting Smad5, thereby weakening Id2-mediated repression of Snail and Twist (Fig. 5).

miRNAs, a class of small noncoding RNAs, are critical regulators of physiological functions but their dysregulation gives rise to a wide spectrum of diseases [26]. miRNAs have been emerging as promising biomarkers and therapeutic targets for PAH [27]. miR-27a, a tumor-related factor [28], has been demonstrated to be increased and promote the proliferation of vascular cells in pulmonary arteries during PAH progression [8–10]. It is well documented that proliferation of vascular cells and/or EndMT contributes greatly to pulmonary arterial remodeling in PAH [3,4]. Therefore, miR-27a could be a therapeutic target for PAH if it promotes EndMT in PAH. This hypothesis has been substantiated in the present study. Right ventricular failure is a serious complication of PAH and accounts for the ultimate death. Interestingly, up-regulation of miR-27a has been observed in transverse aortic constriction-induced cardiac hypertrophy [29], implying that miR-27a would enhance the progression of right ventricular failure in PAH.

BMP signaling is crucial to blood vessel development, but its anomalies underlie many vascular diseases, such as PAH [11]. BMPR II receptor mutation has been identified in PAH patients [12,30]. Dysregulation of BMP signaling has been demonstrated in experimental animals or patients with PAH [13–15], and correction of dysfunctional BMP signaling reverses PAH efficiently [31,32]. Those lines of evidence suggest that maintenance of BMP signaling homeostasis may serve as a therapeutic avenue for PAH. Here, we found that both Smad5 and p-Smad5 were down-regulated in PAECs during hypoxia-induced EndMT. Mechanistically, miR-27a, which was up-regulated by hypoxia, suppressed the translation of Smad5 mRNA by binding to its 3′ UTR. These results suggested that miR-27a suppressed BMP signaling by targeting Smad5, thereby promoting hypoxia-induced EndMT.

Id proteins are a class of basic helix-loop-helix transcription factors. They lack DNA binding domain, and thus act as dominant-negative regulators of transcription [25]. Id1-3 have been found to be down-regulated in PASMCs in monocrotaline-induced and familial PAH [23,33], and Id2 is down-regulated in PASMCs in hypoxia-induced PAH [17]. Nonetheless, the role of Id2 in EndMT during hypoxia-induced PAH has yet to be elucidated. We demonstrated that Id2 was down-regulated in EndMT during hypoxia-induced PAH and attenuated hypoxia-induced EndMT by reducing the expression of Snail and Twist. Id2 has been shown to down-regulate Snail *via* repression of transforming growth factor β signaling [21] and reduce the transcriptional activity and stability of Twist by competitively binding with E-proteins [20,25]. Together with our data, the available evidence suggests that down-regulation of Id2 could be a key trigger of hypoxia-induced EndMT.

5. Conclusion

In summary, the present study has demonstrated that in hypoxia-

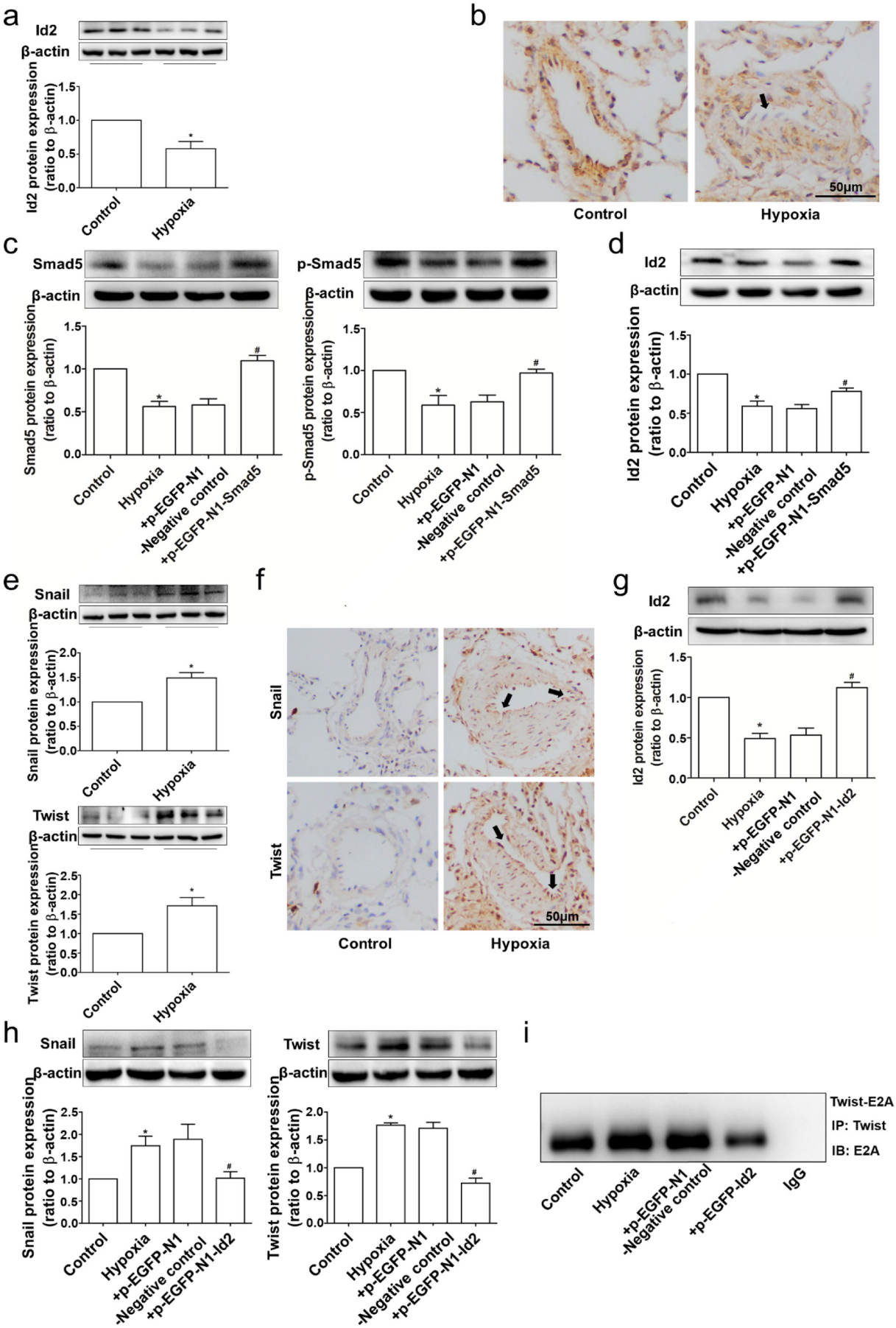

(caption on next page)

Fig. 4. Overexpressing Smad5 up-regulated Id2 and thereby down-regulated Snail and Twist. (a) The expression of Id2 in rat pulmonary artery detected by Western blot (n = 3). (b) The expression of Id2 in rat pulmonary artery detected by immunohistochemistry; the arrows indicated the expression of Id2 in the tunica intima of pulmonary artery. (c) The expression of both Smad5 and p-Smad5 in hypoxia-induced HPAECs after Smad5-expressing plasmids transfection detected by Western blot (n = 3). (d) The expression of Id2 in hypoxia-induced HPAECs after Smad5 overexpression detected by Western blot (n = 3). (e) The expression of both Snail and Twist in rat pulmonary artery detected by Western blot (n = 3). (f) The expression of both Snail and Twist in rat pulmonary artery detected by immunohistochemistry; the arrows indicated the expression of both Snail and Twist in the tunica intima of pulmonary artery. (g) The expression of Id2 in hypoxia-induced HPAECs after Id2-expressing plasmid transfection detected by Western blot (n = 3). (h) The expression of both Snail and Twist in hypoxia-induced HPAECs after Id2 overexpression detected by Western blot (n = 3). (i) The co-immunoprecipitation analysis for examining whether Id2 competes with Twist to bind with E2A. Data are mean ± S.E.M. $*P < 0.05$ compared with Control, $\#P < 0.05$ compared with Hypoxia.

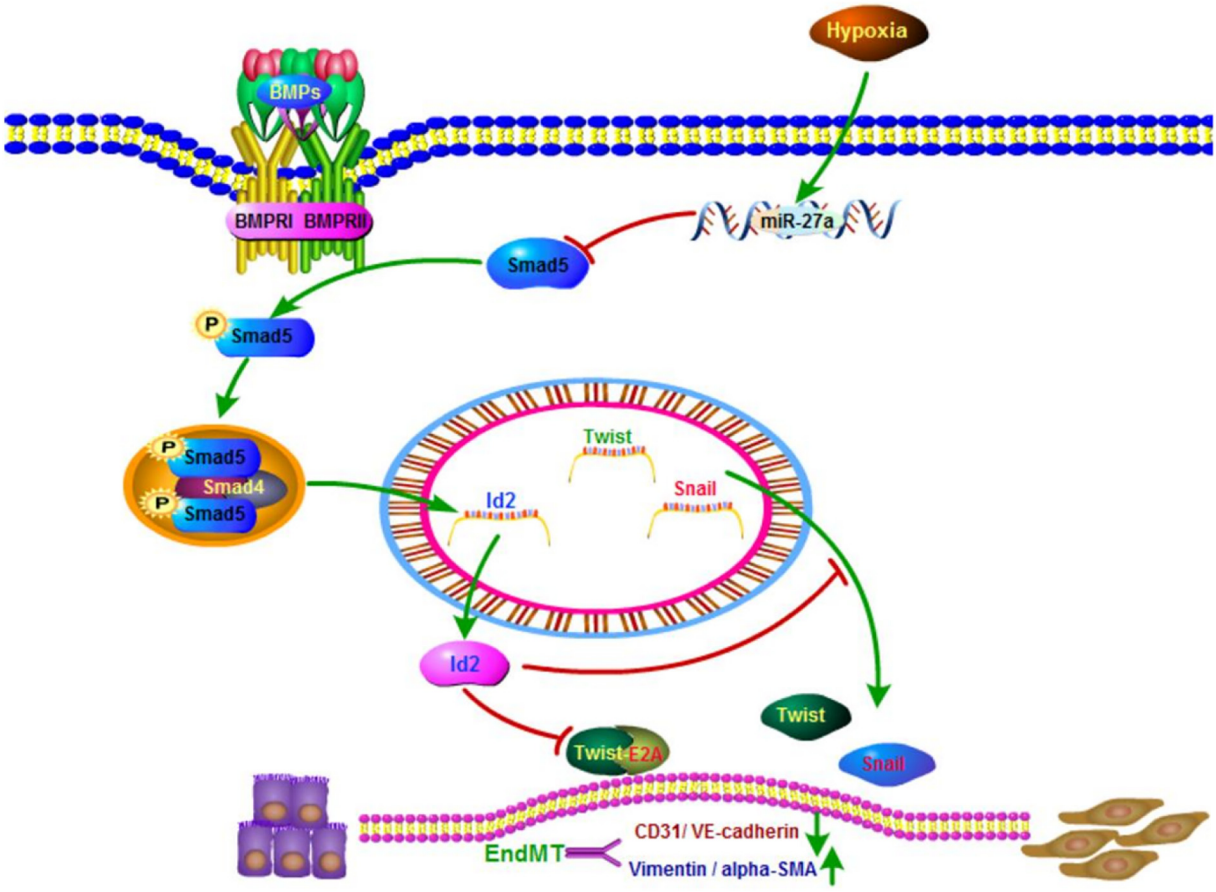

Fig. 5. Schematic diagram of role of miR-27a in endothelial-mesenchymal transition (EndMT) during hypoxia-induced pulmonary arterial hypertension.

induced PAH, up-regulation of miR-27a suppressed BMP signaling by targeting Smad5, and up-regulated Snail and Twist, thereby promoting EndMT. Our data suggest that miR-27a may be a novel therapeutic target for PAH.

Conflict of interest

The authors declare that there are no conflicts of interest.

Acknowledgments

This work was supported by grants from the National Natural Science Foundation of China (No. 91439105, 81473209, 81872872, 91639114, 81570429).

References

[1] M.M. Hoeper, H.J. Bogaard, R. Condliffe, R. Frantz, D. Khanna, M. Kurzyna, D. Langleben, A. Manes, T. Satoh, F. Torres, M.R. Wilkins, D.B. Badesch, Definitions and diagnosis of pulmonary hypertension, J. Am. Coll. Cardiol. 62 (2013) D42–D50.
[2] R.M. Tuder, S.L. Archer, P. Dorfmüller, S.C. Erzurum, C. Guignabert, E. Michelakis, M. Rabinovitch, R. Schermuly, K.R. Stenmark, N.W. Morrell, Relevant issues in the pathology and pathobiology of pulmonary hypertension, J. Am. Coll. Cardiol. 62 (2013) D4–12.
[3] J.S. Grant, K. White, M.R. MacLean, A.H. Baker, MicroRNAs in pulmonary arterial remodeling, Cell. Mol. Life Sci. 70 (2013) 4479–4494.
[4] B. Ranchoux, F. Antigny, C. Rucker-Martin, A. Hautefort, C. Péchoux, H.J. Bogaard, P. Dorfmüller, S. Remy, F. Lecerf, S. Planté, S. Chat, E. Fadel, A. Houssaini, I. Anegon, S. Adnot, G. Simonneau, M. Humbert, S. Cohen-Kaminsky, F. Perros, Endothelial-to-mesenchymal transition in pulmonary hypertension, Circulation 131 (2015) 1006–1018.
[5] D.P. Bartel, MicroRNAs: genomics, biogenesis, mechanism, and function, Cell 116 (2004) 281–297.
[6] B. Qiao, B.-X. He, J.-H. Cai, Q. Tao, A. King-Yin Lam, MicroRNA-27a-3p modulates the Wnt/β-catenin signaling pathway to promote epithelial-mesenchymal transition in oral squamous carcinoma stem cells by targeting SFRP1, Sci. Rep. 7 (2017) 44688.
[7] G. Zeng, W. Xun, K. Wei, Y. Yang, H. Shen, MicroRNA-27a-3p regulates epithelial to mesenchymal transition via targeting YAP1 in oral squamous cell carcinoma cells, Oncol. Rep. 36 (2016) 1475–1482.
[8] B.-Y. Kang, K. Park, J.M. Kleinhenz, T.C. Murphy, R.L. Sutliff, D. Archer, C.M. Hart, Peroxisome proliferator-activated receptor γ regulates the V-Ets avian erythroblastosis virus E26 oncogene homolog 1/microRNA-27a axis to reduce endothelin-1 and endothelial dysfunction in the sickle cell mouse lung, Am. J. Respir. Cell Mol. Biol. 56 (2017) 131–144.
[9] B.-Y. Kang, K.K. Park, D.E. Green, K.M. Bijli, C.D. Searles, R.L. Sutliff, C.M. Hart, Hypoxia mediates mutual repression between microRNA-27a and PPARγ in the pulmonary vasculature, PLoS One 8 (2013) e79503.
[10] X. Xie, S. Li, Y. Zhu, L. Liu, Y. Pan, J. Wang, W. Shi, Y. Song, L. Yang, L. Gao,

W. Zang, M. Li, MicroRNA-27a/b mediates endothelin-1-induced PPARγ reduction and proliferation of pulmonary artery smooth muscle cells, Cell Tissue Res. (2017) 527–539.
[11] J. Cai, E. Pardali, G. Sánchez-Duffhues, P. ten Dijke, BMP signaling in vascular diseases, FEBS Lett. 586 (2012) 1993–2002.
[12] Z. Deng, J.H. Morse, S.L. Slager, N. Cuervo, K.J. Moore, G. Venetos, S. Kalachikov, E. Cayanis, S.G. Fischer, R.J. Barst, S.E. Hodge, J.A. Knowles, Familial primary pulmonary hypertension (gene PPH1) is caused by mutations in the bone morphogenetic protein receptor-II gene, Am. J. Hum. Genet. 67 (2000) 737–744.
[13] B. Girerd, D. Montani, F. Coulet, B. Sztrymf, A. Yaici, X. Jaïs, D. Tregouet, A. Reis, V. Drouin-Garraud, A. Fraisse, O. Sitbon, D.S. O'Callaghan, G. Simonneau, F. Soubrier, M. Humbert, Clinical outcomes of pulmonary arterial hypertension in patients carrying an ACVRL1 (ALK1) mutation, Am. J. Respir. Crit. Care Med. 181 (2010) 851–861.
[14] M. Shintani, H. Yagi, T. Nakayama, T. Saji, R. Matsuoka, A new nonsense mutation of SMAD8 associated with pulmonary arterial hypertension, J. Med. Genet. 46 (2009) 331–337.
[15] G. Wang, R. Fan, R. Ji, W. Zou, D.J. Penny, N.P. Varghese, Y. Fan, Novel homozygous BMP9 nonsense mutation causes pulmonary arterial hypertension: a case report, BMC Pulm. Med. 16 (2016) 17.
[16] R.K. Hopper, J.-R.A.J. Moonen, I. Diebold, A. Cao, C.J. Rhodes, N.F. Tojais, J.K. Hennigs, M. Gu, L. Wang, M. Rabinovitch, In pulmonary arterial hypertension, reduced BMPR2 promotes endothelial-to-mesenchymal transition via HMGA1 and its target slug, Circulation 133 (2016) 1783–1794.
[17] Y. Zeng, H. Liu, K. Kang, Z. Wang, G. Hui, X. Zhang, J. Zhong, W. Peng, R. Ramchandran, J.U. Raj, D. Gou, Hypoxia inducible factor-1 mediates expression of miR-322: potential role in proliferation and migration of pulmonary arterial smooth muscle cells, Sci. Rep. 5 (2015) 12098.
[18] K. Miyazono, K. Miyazawa, Id: a target of BMP signaling, Sci. STKE Signal Transduct. Knowl. Environ. 2002 (2002) pe40.
[19] J. Yang, M. Velikoff, M. Agarwal, S. Disayabutr, P.J. Wolters, K.K. Kim, Overexpression of inhibitor of DNA-binding 2 attenuates pulmonary fibrosis through regulation of c-Abl and twist, Am. J. Pathol. 185 (2015) 1001–1011.
[20] M. Hayashi, K. Nimura, K. Kashiwagi, T. Harada, K. Takaoka, H. Kato, K. Tamai, Y. Kaneda, Comparative roles of Twist-1 and Id1 in transcriptional regulation by BMP signaling, J. Cell Sci. 120 (2007) 1350–1357.
[21] M. Kondo, E. Cubillo, K. Tobiume, T. Shirakihara, N. Fukuda, H. Suzuki, K. Shimizu, K. Takehara, A. Cano, M. Saitoh, K. Miyazono, A role for Id in the regulation of TGF-beta-induced epithelial-mesenchymal transdifferentiation, Cell Death Differ. 11 (2004) 1092–1101.
[22] K. Miyazono, Y. Kamiya, M. Morikawa, Bone morphogenetic protein receptors and signal transduction, J. Biochem. (Tokyo) 147 (2010) 35–51.
[23] J. Yang, R.J. Davies, M. Southwood, L. Long, X. Yang, A. Sobolewski, P.D. Upton, R.C. Trembath, N.W. Morrell, Mutations in bone morphogenetic protein type II receptor cause dysregulation of Id gene expression in pulmonary artery smooth muscle cells: implications for familial pulmonary arterial hypertension, Circ. Res. 102 (2008) 1212–1221.
[24] E. Pardali, G. Sanchez-Duffhues, M.C. Gomez-Puerto, P. Ten Dijke, TGF-β-induced endothelial-mesenchymal transition in fibrotic diseases, Int. J. Mol. Sci. 18 (2017) 2157.
[25] J. Perk, A. Iavarone, R. Benezra, Id family of helix-loop-helix proteins in cancer, Nat. Rev. Cancer 5 (2005) 603–614.
[26] X.-Z. Zou, T. Liu, Z.-C. Gong, C.-P. Hu, Z. Zhang, MicroRNAs-mediated epithelial-mesenchymal transition in fibrotic diseases, Eur. J. Pharmacol. 796 (2017) 190–206.
[27] O. Boucherat, F. Potus, S. Bonnet, microRNA and pulmonary hypertension, Adv. Exp. Med. Biol. 888 (2015) 237–252.
[28] J. Quan, S. Liu, K. Dai, L. Jin, T. He, X. Pan, Y. Lai, MicroRNA-23a/24-2/27a as a potential diagnostic biomarker for cancer: a systematic review and meta-analysis, Mol. Clin. Oncol. 8 (2018) 159–169.
[29] H. Nishi, K. Ono, T. Horie, K. Nagao, M. Kinoshita, Y. Kuwabara, S. Watanabe, T. Takaya, Y. Tamaki, R. Takanabe-Mori, H. Wada, K. Hasegawa, Y. Iwanaga, T. Kawamura, T. Kita, T. Kimura, MicroRNA-27a regulates beta cardiac myosin heavy chain gene expression by targeting thyroid hormone receptor beta1 in neonatal rat ventricular myocytes, Mol. Cell. Biol. 31 (2011) 744–755.
[30] International PPH Consortium, K.B. Lane, R.D. Machado, M.W. Pauciulo, J.R. Thomson, J.A. Phillips, J.E. Loyd, W.C. Nichols, R.C. Trembath, Heterozygous germline mutations in BMPR2, encoding a TGF-beta receptor, cause familial primary pulmonary hypertension, Nat. Genet. 26 (2000) 81–84.
[31] L. Long, M.L. Ormiston, X. Yang, M. Southwood, S. Gräf, R.D. Machado, M. Mueller, B. Kinzel, L.M. Yung, J.M. Wilkinson, S.D. Moore, K.M. Drake, M.A. Aldred, P.B. Yu, P.D. Upton, N.W. Morrell, Selective enhancement of endothelial BMPR-II with BMP9 reverses pulmonary arterial hypertension, Nat. Med. 21 (2015) 777–785.
[32] J. Yang, X. Li, R.S. Al-Lamki, C. Wu, A. Weiss, J. Berk, R.T. Schermuly, N.W. Morrell, Sildenafil potentiates bone morphogenetic protein signaling in pulmonary arterial smooth muscle cells and in experimental pulmonary hypertension, Arterioscler. Thromb. Vasc. Biol. 33 (2013) 34–42.
[33] R.E. Morty, B. Nejman, G. Kwapiszewska, M. Hecker, A. Zakrzewicz, F.M. Kouri, D.M. Peters, R. Dumitrascu, W. Seeger, P. Knaus, R.T. Schermuly, O. Eickelberg, Dysregulated bone morphogenetic protein signaling in monocrotaline-induced pulmonary arterial hypertension, Arterioscler. Thromb. Vasc. Biol. 27 (2007) 1072–1078.